J Stat Phys (2009) 134: 185–206
DOI 10.1007/s10955-008-9668-y

Three-Dimensional Random Voronoi Tessellations: From Cubic Crystal Lattices to Poisson Point Processes

Valerio Lucarini

Received: 18 May 2008 / Accepted: 16 December 2008 / Published online: 7 January 2009

Abstract We perturb the simple cubic (SC), body-centered cubic (BCC), and face-centered cubic (FCC) structures with a spatial Gaussian noise whose adimensional strength is controlled by the parameter α and analyze the statistical properties of the cells of the resulting Voronoi tessellations using an ensemble approach. We concentrate on topological properties of the cells, such as the number of faces, and on metric properties of the cells, such as the area, volume and the isoperimetric quotient. The topological properties of the Voronoi tessellations of the SC and FCC crystals are unstable with respect to the introduction of noise, because the corresponding polyhedra are geometrically degenerate, whereas the tessellation of the BCC crystal is topologically stable even against noise of small but finite intensity. Whereas the average volume of the cells is the intensity parameter of the system and does not depend on the noise, the average area of the cells has a rather interesting behavior with respect to noise intensity. For weak noise, the mean area of the Voronoi tessellations corresponding to perturbed BCC and FCC perturbed increases quadratically with the noise intensity. In the case of perturbed SCC crystals, there is an optimal amount of noise that minimizes the mean area of the cells. Already for a moderate amount of noise ($\alpha > 0.5$), the statistical properties of the three perturbed tessellations are indistinguishable, and for intense noise ($\alpha > 2$), results converge to those of the Poisson-Voronoi tessellation. Notably, 2-parameter gamma distributions constitute an excellent model for the empirical pdf of all considered topological and metric properties. By analyzing jointly the statistical properties of the area and of the volume of the cells, we discover that also the cells shape, measured by the isoperimetric quotient, fluctuates. The Voronoi tessellations of the BCC and of the FCC structures result to be local maxima for the isoperimetric quotient among space-filling tessellations, which suggests a weaker form of the recently disproved Kelvin conjecture. Moreover, whereas the size of the isoperimetric quotient fluctuations go to zero linearly with noise in the SC and BCC case, the decrease is quadratic in the FCC case. Correspondingly, anomalous scaling relations with exponents larger than $3/2$ are observed between the

V. Lucarini
Department of Physics, University of Bologna, Viale Berti Pichat 6/2, 40127 Bologna, Italy

V. Lucarini (✉)
Istituto Nazionale di Fisica Nucleare, Sezione di Bologna, Viale Berti Pichat 6/2, 40127 Bologna, Italy
e-mail: lucarini@adgb.df.unibo.it

area and the volumes of the cells for all cases considered, and, except for the FCC structure, also for infinitesimal noise. In the Poisson-Voronoi limit, the exponent is ∼1.67. The anomaly in the scaling indicates that large cells preferentially feature large isoperimetric quotients. The FCC structure, in spite of being topologically unstable, results to be the most stable against noise when the shape—as measured by the isoperimetric quotient—of the cells is considered. These scaling relations apply only for a finite range and should be taken as descriptive of the bulk statistical properties of the cells. As the number of faces is strongly correlated with the sphericity (cells with more faces are bulkier), the anomalous scaling is heavily reduced when we perform power law fits separately on cells with a specific number of faces.

Keywords Voronoi tessellation · Numerical simulations · Random geometry · Symmetry break · Topological stability · Poisson point process · Cubic crystals · Simple cubic · Face-centered cubic · Body-centered cubic · Gaussian noise · Gamma distribution · Anomalous scaling · Isoperimetric quotient · Fluctuations · Kelvin's conjecture · Kepler's conjecture · Kendall's conjecture

1 Introduction

A Voronoi tessellation [54, 55] is a partitioning of an Euclidean N-dimensional space Ω defined in terms of a given discrete set of points $X \subset \Omega$. For almost any point $a \in \Omega$ there is one specific point $x \in X$ which is closest to a. Some point a may be equally distant from two or more points of X. If X contains only two points, x_1 and x_2, then the set of all points with the same distance from x_1 and x_2 is a hyperplane, which has codimension 1. The hyperplane bisects perpendicularly the segment from x_1 and x_2. In general, the set of all points closer to a point $x_i \in X$ than to any other point $x_j \neq x_i, x_j \in X$ is the interior of a convex $(N-1)$-polytope usually called the Voronoi cell for x_i. The set of the $(N-1)$-polytopes Π_i, each corresponding to—and containing—one point $x_i \in X$, is the Voronoi tessellation corresponding to X. Extensions to the case of non-Euclidean spaces have also been presented [31, 43].

Since Voronoi tessellations boil up to being optimal partitionings of the space resulting from a set of *generating points*, they have long been considered for applications in several research areas, such as telecommunications [47], biology [18], astronomy [27], forestry [5] atomic physics [19], metallurgy [58], polymer science [13], materials science [7, 12, 33], and biophysics [48] In a geophysical context, Voronoi tessellations have been widely used to analyze spatially distributed observational or model output data [35, 36, 52]. In condensed matter physics, the Voronoi cell of the lattice point of a crystal is known as the Wigner-Seitz cell, whereas the Voronoi cell of the reciprocal lattice point is the Brillouin zone [1, 6]. Voronoi tessellations have been used for performing structure analysis for crystalline solids and supercooled liquids [53, 59], for detecting glass transitions [22], for emphasizing the geometrical effects underlying the vibrations in the glass [37], and for performing detailed and efficient electronic calculations [3, 45]. For a review of the theory and applications of Voronoi tessellations, see [2] and [43].

As the theoretical results on the statistical properties of general N-dimensional Voronoi tessellations are still relatively limited, direct numerical simulation constitute a crucial investigative approach. At computational level, the evaluation of the Voronoi tessellation of a given discrete set of points X is not a trivial task, and the definition of optimal procedures is ongoing and involves various scientific communities [4, 8, 21, 50, 56]. The specific and relevant problem of computing the geometric characteristics of Poisson-Voronoi

tessellations has been the subject of intense theoretical and computational effort. Poisson-Voronoi tessellations are obtained starting from for a random set of points X generated as output of a homogeneous (in the considered space) Poisson point process. This problem has a great relevance at practical level because it corresponds, *e.g.*, to studying crystal aggregates with random nucleation sites and uniform growth rates. Exact results concerning the mean statistical properties of the interface area, inner area, number of vertices, etc. of the Poisson-Voronoi tessellations have been obtained for Euclidean spaces [9, 10, 14, 38–41]; an especially impressive account is given by Finch [17]. Moreover, the Kendall's conjecture has recently been proved, *i.e.* large cells, asymptotically, tend to have a spherical shape [25, 26, 29]. Several computational studies on 2D and 3D spaces have found results in agreement with the theoretical findings, and, moreover, have shown that both 2-parameter [30] and 3-parameter [24] gamma distributions fit up to a high degree of accuracy the empirical pdfs of several geometrical characteristics of the cells [49, 60]. The *ab-initio* derivation of the pdf of the geometrical properties of Poisson-Voronoi tessellations have not been yet obtained, except in asymptotic regimes [23], which are, surprisingly, not compatible with the gamma distributions family.

In a previous paper [34], we have analyzed in a rather general framework the statistical properties of Voronoi tessellation of the Euclidean 2D plane. In particular, we have followed the transition from regular triangular, square and hexagonal honeycomb Voronoi tessellations to those of the Poisson-Voronoi case, thus analyzing in a common framework symmetry-break processes and the approach to uniformly random distributions of tessellation-generating points, which is basically realized when the typical displacement becomes larger than the lattice unit vector. This analysis has been accomplished by a Monte Carlo analysis of tessellations generated by points whose regular positions are perturbed through a Gaussian noise. The symmetry break induced by the introduction of noise destroys the triangular and square tessellation, which are structurally unstable, whereas the honeycomb hexagonal tessellation is stable also for small but finite noise. Moreover, independently of the unperturbed structure, for all noise intensities (including infinitesimal), hexagons constitute the most common class of cells and the ensemble mean of the cells area and perimeter restricted to the hexagonal cells coincides with the full ensemble mean, which reinforces the idea that hexagons can be taken as *generic* polygons in 2D Voronoi tessellations.

The reasons why the regular hexagonal tessellation has such peculiar properties of robustness relies on the fact that it is optimal both in terms of perimeter-to-area ratio and in terms of *cost* (see [15, 42]). The *extremal* properties of such a tessellation are clearly highlighted by Karch et al. [28], where it is noted that a Gibbs system of repulsive charges in 2D arranges spontaneously for low temperatures (freezes) as a regular hexagonal crystal. Moreover, a regular hexagonal structure has been found for the Voronoi tessellation built from the spontaneously arranged lattice of hot spots (strongest upward motion of hot fluid) of the Rayleigh-Bènard convective cells, with the compensating downward motion of cooled fluid concentrated on the sides of the Voronoi cells [44].

In this paper we want to extend the analysis performed in [34] to the 3D case, which is probably of wider applicative interest. We consider three cubic crystals covering the 3D Euclidean space, namely the simple cubic (SC), the face-centered cubic (FCC) and the body-centered cubic (BCC) lattices [6]. The corresponding space-filling Voronoi cells of such crystals are the cube, the rhombic dodecahedron, and the truncated octahedron. The cubic crystal system is one of the most common crystal systems found in elemental metals, and naturally occurring crystals and minerals. These crystals feature extraordinary geometrical properties:

- the cube is the only space-filling regular solid;
- the FCC (together with the Hexagonal Close Packed structure) features the largest possible packing fraction—the 1611 Kepler's conjecture has been recently proved by Hales [20];
- the Voronoi cell of BCC has been conjectured by Kelvin in 1887 as being the space-filling cell with the smallest surface to volume ratio, and only recently a very cumbersome counter-example has been given by Wearie and Phelan [57]; moreover, the truncated octahedron is conjectured to have the lowest *cost* among all 3D space-filling cells (see [15]).

Because of its low density, basically due to the low packing fraction, the SC system has a high energy structure and is rare in nature, and it is found only in the alpha-form of Po. The BCC is a more compact system and have a low energy structure, is therefore more common in nature. Examples of BCC structures include Fe, Cr, W, and Nb. Finally, thanks to its extremal properties in terms of packing fraction and the resulting high density, FCC crystals are fairly common and specific examples include Pb, Al, Cu, Au and Ag.

The extremal properties of the BCC structure can basically be interpreted as the fact that the corresponding Voronoi cell defines a natural *discrete* mathematical measure, and imply that truncated octahedra constitute an optimal tool for achieving data compression [16]. Another outstanding property is that the Voronoi cell of the BCC structure, as opposed to SC and FCC, is topologically stable with respect to infinitesimal perturbations to the position of the lattice points [51].

Using an ensemble-based approach, we study the break-up of the symmetry of the SC, BCC and FCC systems and of their corresponding Voronoi tessellations by stochastically perturbing with a space-homogeneous Gaussian noise of parametrically controlled strength the positions of the lattice points x_i, and quantitatively evaluating how the statistical properties of the geometrical characteristics of the resulting 3D Voronoi cells change. The strength of considered perturbation ranges up to the point where typical displacements become larger than the lattice unit vector, which basically leads to the limiting case of the Poisson-Voronoi process. Therefore, our work joins on the analysis of Voronoi cells resulting from infinitesimal (namely, small) perturbations to regular cubic lattices to fully random tessellations.

Our paper is organized as follows. In Sect. 2 we discuss some general properties of the Voronoi tessellations considered, describe the methodology of work and the set of numerical experiments performed. In Sect. 3 we show our results. In Sect. 4 we present our conclusions and perspectives for future work.

2 Theoretical and Computational Issues

2.1 General Properties of Voronoi Tessellations

We consider a random point process characterized by a spatially homogeneous coarse-grained intensity ρ_0, such that the expectation value of the number of points x_i in a generic region $\Gamma \in \mathbb{R}^3$ is $\rho_0|\Gamma|$, where $|\Gamma|$ is the Lebesgue measure of Γ, whereas the fluctuations in the number of points are $\approx \sqrt{\rho_0|\Gamma|}$. If $\rho_0|\Gamma| \gg 1$, we are in the thermodynamic limit and boundary effects are negligible , so that the number of cells of the Voronoi tessellation resulting from the set of points x_i and contained inside Γ is $N_V \approx \rho_0|\Gamma|$.

In this paper we consider perfect crystals, crystals with random dislocations, and sparse points resulting from a spatially homogeneous Poisson process. Perfect crystals are obtained when the probability distribution function (pdf) of the random point process can be expressed as a sum of Dirac masses obeying a discrete translational symmetry. Crystals with

random dislocations are periodical in the statistical sense since the pdf of the point-process is a non-singular Lebesgue measurable function obeying discrete translational symmetry. Finally, the pdf of the homogeneous Poisson point process is constant in space.

Using scaling arguments [34], one obtains that in all cases considered the statistical properties of the Voronoi tessellation are intensive, so that the point density ρ_0 can be scaled to unity, or, alternatively, the domain can be scaled to the Cartesian cube $\Gamma_1 = [0,1] \otimes [0,1] \otimes [0,1]$. We will stick to the second approach. We then define $\mu(Y)(\sigma(Y))$ as the mean value (standard deviation) of the variable Y over the N_V cells for the single realization of the random process, whereas the expression $\langle E \rangle (\delta[E])$, indicates the ensemble mean (standard deviation) of the random variable E. We have that $\langle \mu(V) \rangle$, $\langle \sigma(V) \rangle \propto \rho_0^{-1}$, where V is the volume of the Voronoi cell, $\langle \mu(A) \rangle$, $\langle \sigma(A) \rangle \propto \rho_0^{-2/3}$, where A is the surface area of the Voronoi cell, and $\langle \mu(P) \rangle$, $\langle \sigma(P) \rangle \propto \rho_0^{-1/3}$, where P is the total perimeter of the cell. The proportionality constants depend of the specific random point process considered. Therefore, by multiplying the ensemble mean estimators of the mean and standard deviation of the various geometrical properties of the Voronoi cells times the appropriate power of ρ_0, we obtain universal functions.

Going to the topological properties of the cells, we remind that, since each Voronoi cell is convex, its vertices (v), edges (e), and faces (f) are connected by the simplified Euler-Poincare formula for 3D polyhedra $v - e + f = 2$. Moreover, in a generic solid vertices are trivalent (i.e. given by the intersection of three edges), so that $e = 3/2v$, which implies that $f = 1/2v + 2$, so that the knowledge of the number of vertices of a cell provides a rather complete information about the polyhedron. We then derive an additional general result: in each cell the average number (n) of sides of each face is $n = 2e/f = 3v/f = 6v/(v+2) = 6 - 12/f < 6$, which marks a clear difference with respect to the plane case, where the Euler theorem applies [34].

2.2 Exact Results

We first consider the perfect SC, BCC, and FCC cubic crystals having a total of ρ_0 lattice points per unit volume and ρ_0 corresponding Voronoi cells in Γ_1. Therefore, the length of the side of the cubes of the SC, BCC, and FCC crystals are $\rho_0^{-1/3}$, $2^{1/3}\rho_0^{-1/3}$, and $4^{1/3}\rho_0^{-1/3}$, respectively. Basic Euclidean geometry allows us to fully analyze these structures. The cells of the Voronoi tessellation of the SC crystal are cubes (having 12 edges, 6 faces, 8 trivalent vertices) of side length $\rho_0^{-1/3}$ and total surface area $A = 6\rho_0^{-2/3}$. The cells of the Voronoi tessellation of the BCC crystal are truncated octahedra (having 36 edges, 14 faces, 24 trivalent vertices) of side length $2^{-7/6}\rho_0^{-1/3} \approx 0.4454\rho_0^{-1/3}$ and total surface area $A = 3(1+2\sqrt{3})2^{-4/3}\rho_0^{-2/3} \approx 5.3147\rho_0^{-2/3}$. The cells of the Voronoi tessellation of the FCC crystal are rhombic dodecahedra (having 24 edges, 12 faces, 6 trivalent vertices, 8 tetravalent vertices) of side length $2^{-4/3}\sqrt{3}\rho_0^{-1/3} \approx 0.6874\rho_0^{-1/3}$ and total surface area $A = 3 \cdot 2^{5/6}\rho_0^{-2/3} \approx 5.3454\rho_0^{-2/3}$. The standard isoperimetric quotient $Q = 36\pi V^2/S^3$, which measures the in non-dimensional units the surface-to-volume ratio of a solid ($Q = 1$ for a sphere), is 0.5236, 0.7534, and 0.7405 for the SC, BCC, and FCC structures, respectively.

On the other end of the "spectrum of randomness", exact results have been obtained on Poisson-Voronoi tessellations using rather cumbersome analytical tools. We report some of the results discussed by Okabe et al. [43] and Finch [17]:

- the average number of vertices is $\langle \mu(v) \rangle = \frac{96\pi^2}{35} \approx 27.0709$ and its standard deviation is $\langle \sigma(v) \rangle \approx 6.6708$; exploiting the Euler-Poincare relation plus the genericity property, we

obtain $\langle\mu(e)\rangle = 3/2\langle\mu(v)\rangle$, $\langle\mu(f)\rangle = 1/2\langle\mu(v)\rangle + 2$, $\langle\sigma(e)\rangle = 3/2\langle\sigma(v)\rangle$, and $\langle\sigma(f)\rangle = 1/2\langle\sigma(v)\rangle$;

- the average surface area is $\langle\mu(A)\rangle = (\frac{256\pi}{3})^{1/3}\Gamma(\frac{5}{3})\rho_0^{-2/3} \approx 5.8209\rho_0^{-2/3}$ (with $\Gamma(\cdot)$ here indicating the usual Gamma function), and its standard deviation is $\langle\sigma(A)\rangle \approx 1.4804\rho_0^{-2/3}$;
- the average volume is, by definition, $\langle\mu(V)\rangle = \rho_0^{-1}$, whereas its standard deviation is $\langle\sigma(V)\rangle \approx 0.4231\rho_0^{-1}$.

2.3 Simulations

For the SC, BCC, and FCC lattices, we introduce a symmetry-breaking 3D-homogeneous ε-Gaussian noise, which randomizes the position of each of the points x_i about its deterministic position with a spatial variance $|\varepsilon^2|$. By defining $|\varepsilon^2| = \alpha^2/\rho_0^{2/3} = \alpha^2 l_Q^2$, thus expressing the mean squared displacement as a fraction α^2 of the inverse of the 2/3rd power of the density of points, which is the natural squared length scale l_Q^2. The parameter α^2 can be loosely interpreted as a normalized temperature of the lattice. Note that in all cases, when ensembles are considered, the distribution of the x_i is still periodic. The statistical analysis is performed over 100-members ensembles of Voronoi tessellations generated for all values of α ranging from 0 to 2 with step 0.01, plus additional values aimed at checking the weak- and high-noise limits. Another set of simulations is performed by computing an ensemble of 100 Poisson-Voronoi tessellations generated starting from a set of uniformly randomly distributed ρ_0 points per unit volume.

The actual simulations are performed by applying, within a customized routine, the `MATLAB7.0®` functions `voronoin.m` and `convhulln.m`, which implement the algorithm introduced by Barber et al. [4], to a set of points x_i having coarse grained density $\rho_0 = 100000$ and generated according to the considered random process. The function `voronoin.m` associates to each point the vertices of the corresponding Voronoi cell and its volume, whereas the function `convhulln.m` is used to generate the convex hull of the cell.

Note that the convex hull is given in terms of 2-simplices, *i.e.* triangles. Whereas this information is sufficient for computing the total surface area of the cell, an additional step is needed in order to define the topological properties of the cell. In fact, in order to determine the actual number of faces of the cell and define exactly what polygon each face is, we need to explore whether neighbouring simplices are coplanar, and thus constitute higher order polygons. This is accomplished by computing the unit vector $\hat{i}_k$ orthogonal to each simplex s_k and computing the matrix of the scalar products $\langle\hat{i}_j, \hat{i}_k\rangle$ for all the simplices of the cell. When the scalar products $\langle\hat{i}_p, \hat{i}_q\rangle$, $m \leq p, q \leq m+n-1$ of unit vectors orthogonal to n neighbouring simplices s_k $m \leq k \leq m+n-1$ are close to 1—within a specified tolerance ξ, corresponding to a tolerance of about $\sqrt{2\xi}$ in the angle between the unit vector—we have that $\bigcup_{k=m}^{m+n-1} s_k$ is a polygon with $n+2$ sides. We have consistently verified that choosing any tolerance smaller than $\xi = 10^{-8}$ we obtain basically the same results.

Other values of ρ_0—smaller and larger than $\rho_0 = 1000000$—have been used in order to check the previously described scaling laws, which are found to be precisely verified in all numerical experiments. The benefit of using such a large value of ρ_0 relies on the fact that fluctuations in the ensembles are quite small. Tessellation has been performed starting from points x_i belonging to the square $[-0.1, 1.1] \otimes [-0.1, 1.1] \otimes [-0.1, 1.1] \supset \Gamma_1 = [0, 1] \otimes [0, 1] \otimes [0, 1]$, but only the cells belonging to Γ_1 have been considered for evaluating the statistical properties. Since the external shell having a thickness of 0.1 comprises about 10 layers of cells, boundary effects due to one-step Brownian diffusion of the points nearby the boundaries, which, in the case of large values of α, cause ρ_0 depletion, become negligible.

3 From Regular to Random Lattices

By definition, if $\alpha = 0$ we are in the deterministic case of SC, BCC, and FCC lattices. We study how the geometrical properties of the Voronoi cells change with α, covering the whole range going from the symmetry break, occurring when α becomes positive, up to the progressively more and more uniform distribution of x_i, obtained when α is large with respect to 1 and the pdfs of nearby points x_i overlap more and more significantly.

3.1 Faces, Edges, Vertices

When spatial noise is present in the system, the resulting Voronoi cells are generic polyhedra, so that degenerate quadrivalent vertices, such as those present in the rhombic dodecahedron [51] are removed with probability 1. Therefore, we expect that $\langle \mu(e) \rangle = 3/2 \langle \mu(v) \rangle$, $\langle \mu(f) \rangle = 1/2 \langle \mu(v) \rangle + 2$, $\langle \sigma(e) \rangle = 3/2 \langle \sigma(v) \rangle$, and $\langle \sigma(f) \rangle = 1/2 \langle \sigma(v) \rangle$. These relations have been verified up to a very high degree of accuracy in our simulations, so that, in order to describe the topology of the cell, it is sufficient to present the statistical properties of just one among e, f, and v. In Fig. 1 we present our results relative to the number of faces of the Voronoi cells.

In the case of the SC and FCC crystals, a minimal amount of symmetry-breaking noise impacts as a singular perturbation the statistical properties of $\mu(f)$ and $\sigma(f)$, since $\langle \mu(f) \rangle$ and $\langle \sigma(f) \rangle$ are discontinuous in $\alpha = 0$. In the SC case, the average number of faces jumps from 8 to slightly above 16, whereas, as shown in [51], the disappearance of the quadrivalent vertices in the rhombic dodecahedron case (FCC crystal) causes an increase of two units (up to exactly 14) in the average number of faces. Near $\alpha = 0$, for both SC and FCC perturbed crystals $\langle \mu(f) \rangle$ depends linearly on α as $\langle \mu(f) \rangle \approx \langle \mu(f) \rangle|_{\alpha=0+} + \gamma\alpha$, where by $\langle \cdot \rangle|_{\alpha=0+}$

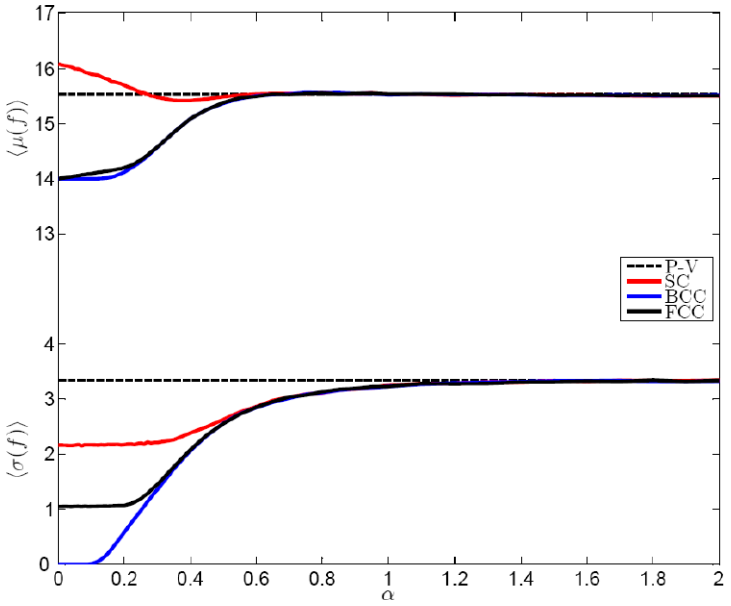

Fig. 1 Ensemble mean of the mean and of the standard deviation of the number of faces (f) of the Voronoi cells for perturbed SC, BCC and FCC cubic crystals. The error bars, whose half-width is twice the standard deviation computed over the ensemble, are too small to be plotted. The Poisson-Voronoi limit is indicated

we mean the limit for infinitesimal noise of the quantity $\langle\cdot\rangle$. The proportionality constant has opposite sign in the two cases, with $\gamma \approx -1.5 \pm 0.05$ for the SC and $\gamma \approx 1 \pm 0.05$ for the FCC case.

Moreover, the introduction of noise generates the sudden appearance of a finite standard deviation in the number of faces in each cell $\langle\sigma(f)\rangle|_{\alpha=0+}$, which is larger for SC crystals. In the case of FCC crystals, Troadec et al. [51] propose a theoretical value $\langle\sigma(f)\rangle|_{\alpha=0+} = \sqrt{4/3}$, whereas our numerical estimate is about 10% lower, actually in good agreement with the numerical results presented by Troadec et al. in the same paper. Somewhat surprisingly, the $\langle\sigma(f)\rangle$ is almost constant for a finite range near $\alpha = 0$ ranging up to about $\alpha \approx 0.3$ for the SC crystal and $\alpha \approx 0.2$ for the FCC crystal, thus defining an intrinsic width of the distribution of faces for a—well-defined—"weakly perturbed" state. In the case of the perturbed FCC crystals, in such a range of weak noise we only observe cells having 12 up to 18 faces: this defines the range of applicability of the weak noise linear perturbation analysis by Troadec et al. [51].

When considering the BCC crystal, the impact of introducing noise in the position of the points x_i is rather different. Results are also shown in Fig. 1. Infinitesimal noise does not effect at all the tessellation, in the sense that all Voronoi cells are 14-faceted (as in the unperturbed state). Moreover, even finite-size noise basically does not distort cells in such a way that other polyhedra are created. We have not observed—also going to higher densities—any non-14 faceted polyhedron for up to $\alpha \approx 0.1$ in any member of the ensemble, so that $\langle\mu(f)\rangle = 14$ and $\langle\sigma(f)\rangle = 0$ in a finite range. However, since the Gaussian noise we are using induces for each point x_i a distribution with—an unrealistic—non-compact support, in principle it is possible to have outliers that, at local level, can distort heavily the tessellation, so that we should interpret this result as that finding non 14-faceted cells is highly—in some sense, exponentially—unlikely.

In Fig. 1 the Poisson-Voronoi limiting case is indicated; our simulations provide results in perfect agreement with the analytical result by Okabe et al. [43] and Finch [17]. For $\alpha > 1$ the value of $\langle\mu(f)\rangle$ and $\langle\sigma(f)\rangle$ of the Voronoi tessellations of the three perturbed crystals asymptotically converge to what resulting from the Poisson-Voronoi tessellation, as expected. We should note, though, that in the 2D case the asymptotic convergence has been shown to be much slower [34], so that spatial noise in 3D seems to mix things up much more efficiently. Similarly to the 2D case, the perturbed tessellations are statistically undistinguishable—especially those resulting from the BCC and FCC distorted lattices—well before converging to the Poisson-Voronoi case, thus pointing at some general behavior.

Additional statistical properties of the distribution of the number of faces in the Voronoi tessellation need to be mentioned. The mode of the distribution is quite interesting since the number of faces is, obviously, integer. In the FC and BCC cases, up to $\alpha \approx 0.3$ the mode is 14, whereas for larger values of α 15-faceted polyhedra are the most common ones. Also the Voronoi tessellations of medium-to—highly perturbed SC crystals are dominated by 15-faceted polyhedra, whereas 16-faceted polyhedra dominate up to $\alpha \approx 0.25$.

We also wish to mention that, in broad agreement with previous studies [30, 34, 49, 60], for all non-singular cases—$\alpha > 0$ for SC and FCC crystals, $\alpha > 0.1$ for BCC crystals—, and *a fortiori* for the Poisson-Voronoi case, the distribution of faces f can be represented up to a very high degree of precision with a 2-parameter gamma distribution:

$$g(f|k,\theta) = N_V f^{k-1} \frac{\exp[-f/\theta]}{\theta^k \Gamma(k)}, \tag{1}$$

where $\Gamma(k)$ is the usual gamma function and $N_V \approx \rho_0$ is, by definition, the normalization factor. We remind that $\mu(f) = k(f)\theta(f)$ and $\sigma(f)^2 = k(f)\theta(f)^2$, so that all information

regarding $k(f)$ and $\theta(f)$ can be deduced from Fig. 1. In particular, in the Poisson-Voronoi case, our results are in excellent agreement with those of Tanemura [49]. As a side note, we mention that in such a limit case, we observe cells with number of faces ranging from 6 to 36. Whereas the problem of assessing precisely the goodness of fit of the gamma distribution is a highly debated and crucial one, it is not central in the present paper, so that it will be discussed elsewhere.

Since, as previously discussed, the inverse of number of faces $y = 1/f$ is related to the average number n of sides per face in each Voronoi cell as $n = 6 - 12/f = 6 - 12y$, expression (1) can in principle be used also for studying the statistical properties of n and for finding explicitly, with a simple change of variable, the corresponding n distribution.

In the Poisson-Voronoi limit, Okabe et al. [43] and Finch [17], using some results by Møller [40]—report $\langle\mu(n)\rangle = \langle\mu(2e/f)\rangle = 6 - 12\langle\mu(1/f)\rangle = 144\pi^2/(24\pi^2 + 35) \approx 5.228$ as an exact result. Since they also report $\langle\mu(e)\rangle = 288\pi^2/35 \approx 40.606$ and $\langle\mu(f)\rangle = 48\pi^2/35 + 2 \approx 15.535$, a simple algebraic rearrangement leads to $2\langle\mu(e)\rangle/\langle\mu(f)\rangle = \langle\mu(2e/f)\rangle$ and $6 - 12\langle\mu(1/f)\rangle = 6 - 12/\langle\mu(f)\rangle$, which implies that $1/\langle\mu(f)\rangle = \langle\mu(1/f)\rangle$. It is somewhat puzzling to find that the theory predicts that the mean of the inverse of the number of faces is exactly equal to the inverse of the mean. Actually, our direct numerical simulations give $\langle\mu(2e)\rangle/\langle\mu(f)\rangle = 6 - 12/\langle\mu(f)\rangle \approx 5.228$, with a standard deviation of the ensemble of $5 \cdot 10^{-4}$, whereas by looking at the correct—in the probability measure defined by the homogeneous Poisson point process—statistical estimator (which takes into consideration the correlation of the variables) we have $\langle\mu(n)\rangle = \langle\mu(2e/f)\rangle = 6 - 12\langle\mu(1/f)\rangle \approx 5.189$ with $\delta(\mu(n)) = 5 \cdot 10^{-4}$. Therefore, it seems reasonable to call for a revision of the theoretical calculation, probably focusing on the definition of the probability measure used in the integration.

Note that if we adopt a 2-parameter gamma model for the Poisson-Voronoi data (see expression (2)), fit the parameters with a maximum likelihood (and not a moment-based) method, and then compute analytically $\langle\mu(n)\rangle$, we obtain an almost exact result:

$$\langle\mu(n)_\Gamma\rangle = 6 - 12\langle\mu(1/f)_\Gamma\rangle = 6 - \langle 12/(k-1)\theta\rangle = 5.189, \tag{2}$$

with standard deviation of the ensemble $\approx 5 \cdot 10^{-4}$, where the pedix Γ refers to the fact that we have adopted the 2-parameter gamma statistical model. Instead, we have that, correspondingly, $6 - 12/\langle\mu(f)_\Gamma\rangle = 6 - \langle 12/k\theta\rangle = 5.228$, again with standard deviation of the ensemble $\approx 5 \cdot 10^{-4}$. The same applies also for all considered values of α and for the three perturbed crystalline structures considered in this study. This further reinforces the idea that 2-parameter gamma family pdfs should be thought as excellent statistical models for the distributions of number of faces in general Voronoi tessellations.

3.2 Area and Volume of the Cells

The statistical properties of the area and of the volume of the Voronoi tessellations of the perturbed cubic crystals have a less pathological behavior with respect to what previously described when noise is turned on, as all properties are continuous and differentiable in $\alpha = 0$. Still, some rather interesting features can be observed.

As mentioned above, the ensemble mean of the mean volume of the cells is set to ρ_0^{-1} in all cases, so that we discuss the properties of the ensemble mean $\langle\sigma(V)\rangle$, shown in Fig. 2. We first observe that for all cubic structures the standard deviation converges to zero with vanishing noise, thus meaning that small variations in the position in the lattice points do not create dramatic rearrangements in the cells when their volumes are considered. Moreover,

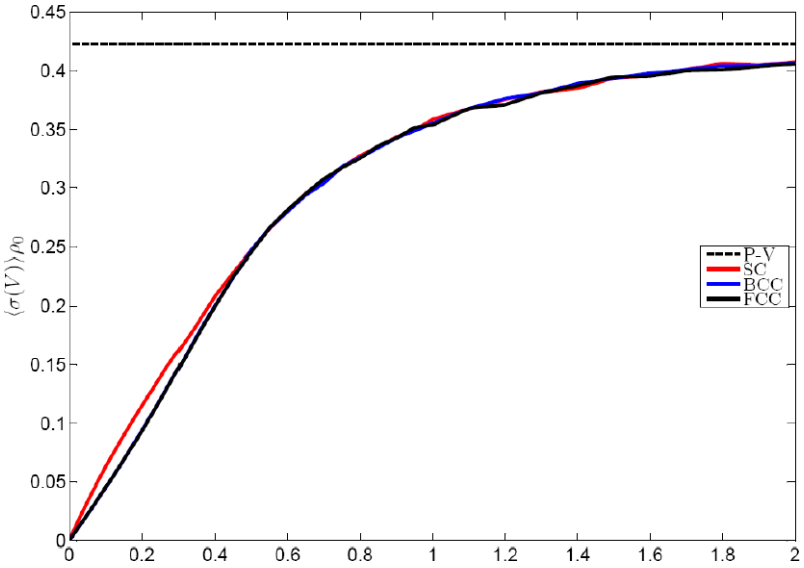

Fig. 2 Ensemble mean of the standard deviation of the volume (V) of the Voronoi cells for perturbed SC, BCC and FCC cubic crystal. The ensemble mean of the mean is set to the inverse of the density. The mean values is Values are multiplied times the appropriate power of the density in order to obtain universal functions. The error bars, whose half-width is twice the standard deviation computed over the ensemble, are too small to be plotted. The Poisson-Voronoi limit is indicated

for $\alpha < 0.3$, a well-defined linear behavior $\langle \sigma(V) \rangle \approx \alpha \mathrm{X}$ is observed for all SC, BCC, and FCC structures. The proportionality constant X is not distinguishable between the BCC and the FCC perturbed crystals, and actually $\mathrm{X} \approx \langle \sigma(V) \rangle_{PV}$, where the pedix refers to the asymptotic Poisson-Voronoi value; the SC curve is somewhat steeper near the origin. The three curves become undistinguishable for $\alpha > 0.4$, so when the noise is moderately intense and reticules are still relatively organized. As previously observed, this seems to be a rather general and robust feature. It is also interesting to note that the attainment of the Poisson-Voronoi limit is quite slow, as compared to the case of the statistical properties of the number of faces of the cell, and a comparable agreement is obtained only for $\alpha > 3$ (not shown).

When considering the area of the cells (see Fig. 3), further interesting properties can be highlighted. First, the behaviour of the ensemble mean $\langle \sigma(A) \rangle$ is rather similar to what just discussed for $\langle \sigma(V) \rangle$. Nevertheless, in this case the agreement between the three perturbed structure is more precisely verified—the three curves are barely distinguishable for all values of α. Moreover, we again observe a linear behavior like $\langle \sigma(A) \rangle \approx \alpha \langle \sigma(A) \rangle_{PV}$, which suggests that the systems closely "align" towards Poisson-like randomness for small values of α. This closely mirror what observed in the 2D case for the expectation value of the standard deviation of the perimeter and of the area of the Voronoi cells [34].

The properties of $\langle \mu(A) \rangle$ for the perturbed crystal structures are also shown in Fig. 3. A striking feature is that, similarly to what noted in the case of triangular and square tessellations of the plane, there is a specific amount of noise that optimizes the mean surface for the perturbed SC crystals. We see that the mean area of the cells decreases by about 8% when α is increased from 0 to about 0.3, where a (quadratic) minimum is attained. For stronger noise, the mean area of the Voronoi cells of the perturbed SC crystals decreases, and, for $\alpha > 0.5$, the asymptotic value of the Poisson-Voronoi tessellation is reached. In terms of cell

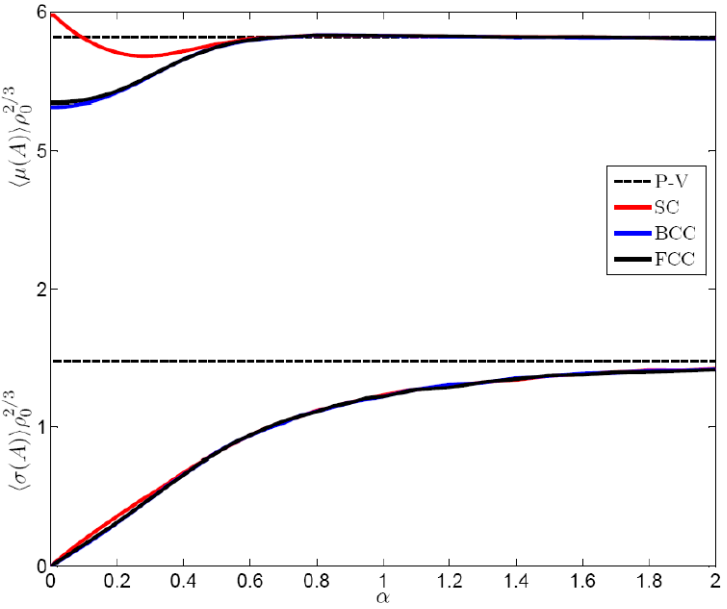

Fig. 3 Ensemble mean of the mean and of the standard deviation of the area (A) of the Voronoi cells for perturbed SC, BCC and FCC cubic crystals. Values are multiplied times the appropriate power of the density in order to obtain universal functions. The error bars, whose half-width is twice the standard deviation computed over the ensemble, are too small to be plotted. The Poisson-Voronoi limit is indicated

surface minimization, the unperturbed cubic tessellation is about 3% worse than the "most random" tessellation.

The dependence of $\langle\mu(A)\rangle$ with respect to α is very interesting also for the perturbed BCC and FCC cubic crystals. In both cases, the mean area increases quadratically (with very similar coefficient) for small values of α, which shows that the Voronoi tessellations of the BCC and FCC cubic crystals are local minima for the mean surface in the set of space-filling tessellations. We know that neither the truncated octahedron nor the rhombic dodecahedron are global minima, since (at least) the Weaire-Phelan structure has a smaller surface [57]. It is reasonable to expect that a similar quadratic increase of the average surface should be observed when perturbing with spatial Gaussian noise the crystalline structure corresponding to the Weaire-Phelan cell. For $\alpha > 0.3$, the values of $\langle\mu(A)\rangle$ for perturbed BCC and FCC crystals basically coincide, and for $\alpha > 0.5$ the Poisson-Voronoi limit is reached within a high accuracy.

As a side note, we mention that, in agreement with several results presented in the introduction, in the case of cells area and volume, for $\alpha > 0$, the empirical pdfs can be represented very efficiently using 2-parameter gamma distributions. This will be analyzed in detail elsewhere.

3.3 Shape of the Cells

The analysis of the properties of the joint area-volume pdf for the Voronoi cells of the considered tessellations sheds light on the statistics of fluctuations of these quantities.

A first interesting statistical property where the joint cells area-volume pdf has to be considered is the isoperimetric quotient $Q = 36\pi V^2/S^3$. The quantity Q is strictly positive and

smaller than 1 for 3D objects, where 1 is realized in the optimal case given by the sphere. Instead, Q is zero for any object with Hausdorff dimension smaller than 3. When evaluating the expectation value of the mean isoperimetric quotient of an ensemble of Voronoi tessellation, we have:

$$\langle \mu(Q) \rangle = 36\pi \langle \mu(V^2/A^3) \rangle \neq 36\pi \langle \mu(V) \rangle^2 / \langle \mu(A) \rangle^3. \tag{3}$$

The presence of fluctuations implies that testing the *average sphericity*—which is basically what Q measures—of a random tessellation is a slightly different problem from testing the average surface for a given average volume, which is what Fig. 3 refers to, whereas in regular tessellations the two problems are equivalent. In Fig. 4 we present our results for the three perturbed crystal structures. In agreement with what observed in Fig. 3, we have that by optimally tuning the intensity of the noise ($\alpha \approx 0.3$) perturbing the SC crystal, $\langle \mu(Q) \rangle$ reaches a maximum, whereas the isoperimetric quotient of the perturbed FCC and BCC crystals has a local maximum for vanishing noise and is monotonically decreasing with α. For $\alpha \geq 0.5$, the value of $\langle \mu(Q) \rangle$ basically coincides for the three perturbed crystalline structures, so that agreement is obtained well before the Poisson-Voronoi limit is attained. It is notable, and counterintuitive, that in the case of the regular SC crystal the isoperimetric quotient is lower than the value of $\langle \mu(Q) \rangle$ obtained in the Poisson-Voronoi limit.

In order to analyze the variability of shape of the cells, we have also analyzed $\langle \sigma(Q) \rangle$, namely the ensemble average of the standard deviation of the isoperimetric quotient. Results are also depicted in Fig. 4. We observe that for all perturbed crystalline structures the variability of the isoperimetric quotient increases with the intensity of noise, as suggested by intuition. This does not tell us much more than what could be derived from the inspection

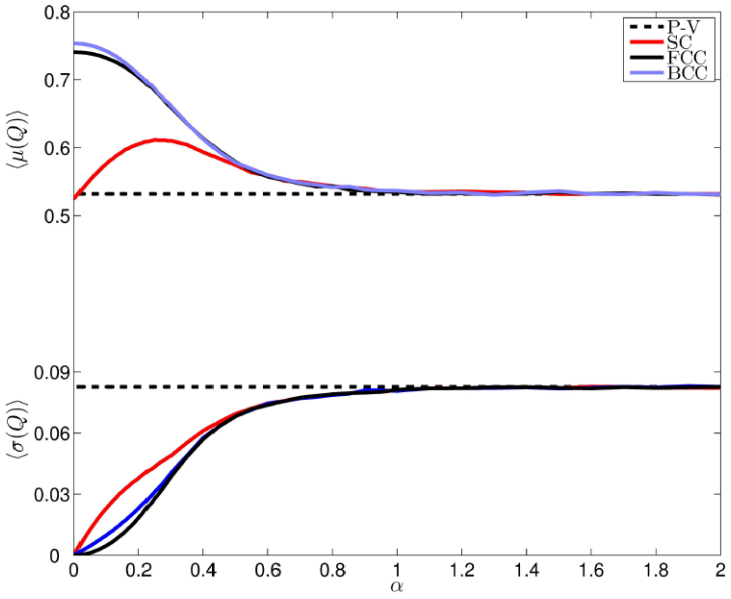

Fig. 4 Ensemble mean of the mean and of the standard deviation (see the different scales) of the isoperimetric quotient $Q = 36\pi V^2/A^3$ of the Voronoi cells for perturbed SC, BCC and FCC cubic crystals The error bars, whose half-width is twice the standard deviation computed over the ensemble, are too small to be plotted. The Poisson-Voronoi limit is indicated. Details in the text

of Figs. 2 and 3. More interesting features appear when considering specifically the weak noise limit of $\langle\sigma(Q)\rangle$. For all of the three perturbed crystals, $\langle\sigma(Q)\rangle|_{\alpha=0+} = 0$, again, consistently with what shown in Figs. 2 and 3. Nevertheless the way such limit is approached varies considerably. In the SC and BCC case, for small values of α, a well-defined linear behavior $\langle\sigma(Q)\rangle \approx \alpha \mathrm{X}$ is observed, with a much larger coefficient for the SC case than in the FCC case, where $\mathrm{X}_{BCC} \approx \langle\sigma(Q)\rangle_{PV} \approx \mathrm{X}_{SC}/3$. Instead, in the FCC case, the approach to 0 of $\langle\sigma(Q)\rangle$ is quadratic, so that for small values of α we have that $\langle\sigma(Q)\rangle \approx \alpha^2 Y$. Therefore, the FCC structure preserves the shape of its cells much more efficiently when noise is introduced. Note that what observed in the weak noise limit is confirmed qualitatively for all values of α, as we always have $\langle\sigma(Q)\rangle_{FCC} < \langle\sigma(Q)\rangle_{BCC} < \langle\sigma(Q)\rangle_{SC}$. For $\alpha \geq 0.5$ the results for the SC, FCC and BCC crystals basically agree and converge to the Poisson-Voronoi limit for $\alpha \geq 1$. Therefore, whereas the Voronoi tessellation of the BCC crystal is the most stable against noise when the topological properties of the cells are considered (see Fig. 1), when analyzing the shape of the cells from a metrical point of view, the FCC crystal is actually the most stable.

In order to further clarify the variability of the shapes of the cells, we take advantage of a strategy of investigation commonly adopted for studying Voronoi tessellations, i.e. the stratification of the expectation values of the geometrical properties with respect to classes defined by the number of sides of the cells [23, 34, 60]. In the present case, it would be profitable to study quantities such as $\langle\mu(V)\rangle|_f$ and $\langle\mu(A)\rangle|_f$, where the pedix indicates that the averages are performed only on cells with f faces. It is readily observed that, in all cases, both $\langle\mu(V)\rangle|_f$ and $\langle\mu(A)\rangle|_f$ increase with f (not shown), for the basic and intuitive reason that cells with a larger number of faces are typically larger in volume and have larger areas. Moreover, and this is a more interesting point, (typically large) cells with a large number of faces have typically a large isoperimetric quotient Q, which makes sense in the context of Kendall's conjecture [23, 25, 26, 29]. In Figs. 5(a), (b), and (c) we present the expectation value of the isoperimetric quotient $\langle\mu(Q)\rangle|_f$ as a function of α for the three perturbed cubic crystals. We observe that in all cases, for a given value of α, $\langle\mu(Q)\rangle|_f$ increases significantly with f, thus confirming the geometrical intuition. Moreover, whereas in the BCC and FCC case $\langle\mu(Q)\rangle|_f$ for a given f decreases monotonically with α, in the SC perturbed crystal for all values of f we have an increase of $\langle\mu(Q)\rangle|_f$ with α up to $\alpha \approx 0.3$. For $\alpha > 1$ the results of the three perturbed crystals tend to converge to the Poisson-Voronoi limit. Therefore, in all considered cases the kind of dependence of the average isoperimetric quotient $\langle\mu(Q)\rangle$ with respect to noise observed in Fig. 4 is realized also in each class of cells as defined by the f label. At any rate, the main additional information contained in Figs. 5 is that for all perturbed crystal structures the number of faces acts as a very good proxy variable for the isoperimetric quotient, and for the shape of the cells.

3.4 Fluctuations and Anomalous Scaling

As discussed above, the areas and the volumes of the Voronoi cells resulting from a random tessellations cells are highly variable. See Fig. 6 for the joint cells area-volume distribution in the case of Poisson-Voronoi tessellation. All considered perturbed crystal structures give qualitatively similar results, but feature, as obvious from the previous discussion, more peaked distributions. In particular, by integrating the 2D distribution along either direction, we obtain a 1D-pdf which, as previously discussed, can closely approximated with a 2-parameter gamma distribution.

If the space is tessellated with finite-size cells which are geometrically similar, their shape determines Q and, consequently, the constant $\varepsilon = \sqrt{Q/36\pi}$ such that for each cell

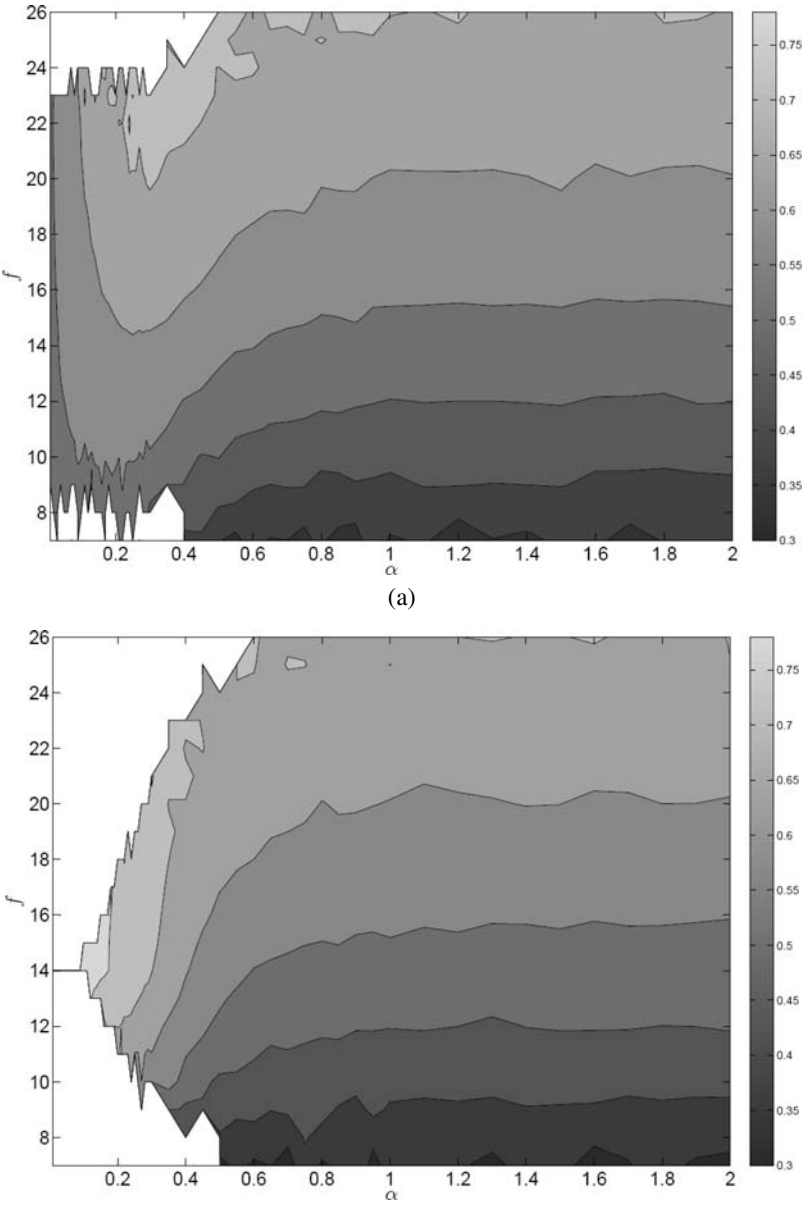

Fig. 5 Ensemble mean of the isoperimetric quotient $\langle \mu(Q) \rangle|_f$ of the Voronoi cells for perturbed SC (**a**), BCC (**b**) and FCC (**c**) cubic crystals, where averages are taken over cells having f faces. A white shading indicates that the corresponding ensemble is empty. Cells with a larger number of faces are typically bulkier

indexed by j we have $V_j = \varepsilon A_j^{3/2}$, where in general $0 < \varepsilon < \sqrt{1/36\pi}$, where the first inequality excludes the possibility of fractal objects and the second inequality implies that no tessellations can *beat* spheres. As we have seen, in the considered Voronoi tessellations the cells are definitely not similar, with larger (and more faceted) cells associated to larger

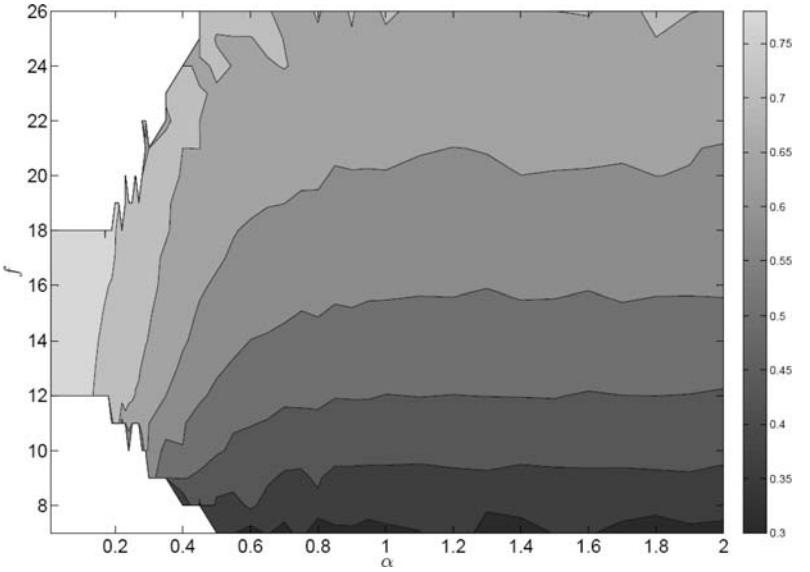

(c)

Fig. 5 (*Continued*)

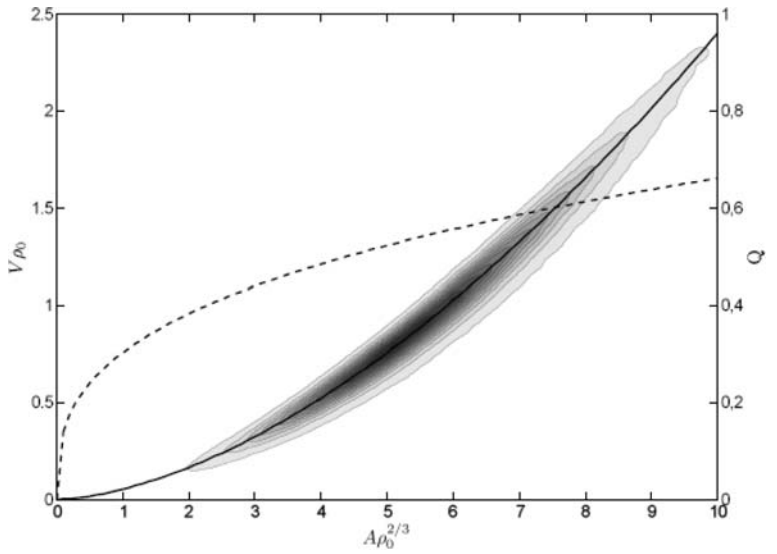

Fig. 6 Joint distribution of the area and of the volume of the Voronoi cells in the Poisson-Voronoi tessellation limit. The *black solid line* indicates the best log-log least squares fit, with ensemble mean of the exponent $\langle \eta \rangle = 3/2 + \langle \eta' \rangle = 1.67$. The *dashed black line* reports the corresponding fit of isoperimetric quotient (see right vertical axis), which scales with the area with exponent $2\langle \eta' \rangle = 0.34$. The effective range of applicability of the scaling law is between 2 and 10 in units of normalized area. Correspondingly, Q ranges between 0.35 and 0.65, and ε between 0.056 and 0.076. Details in the text

isoperimetric quotients. In order to quantify this, we take the following approach. We consider the possibility of a scaling law approximating the (statistical) relationship between the volume and the area of the cells of the form $V(A) = \varepsilon(A)A^{3/2}$ with $\varepsilon(A) = \varepsilon' A^{\eta'}$, so that, if $\eta' > 0$, $\varepsilon(A)$ is monotonically increasing with A. It should be mentioned that this parameterization of $\varepsilon(A)$ amounts to defining Q as $Q(A) = 36\pi\varepsilon'^2 A^{2\eta'}$. Note also for all values of A the constraint $0 \leq \varepsilon(A) < \sqrt{1/36\pi}$ holds, so that the proposed (anomalous) scaling law makes sense at most in the limited range $0 < A < (1/36\pi\varepsilon'^2)^{1/2\eta'}$.

Therefore, in each generated tessellation we attempt a power law fit between the area and the volume of the individual cells as $V_j \approx \varepsilon' A_j^{\eta}$ with $\eta = 3/2 + \eta'$, by performing a linear regression between the logarithm of the volume and of the area of cells. Therefore, given how weight is calculated in the regression, we implicitly define an effective limited range where scaling applies, which corresponds to the interval of A values corresponding to the bulk of the statistics of the cells. Such an interval is, by definition, always included within the largest possible interval $0 < A < (1/36\pi\varepsilon'^2)^{1/2\eta'}$. A corresponding range of values of $\varepsilon(A)$ and of $Q(A)$ is then obtained. We then take the ensemble average for the exponent η among the equivalent tessellations. The values of the best fit for $\langle\eta\rangle$ for the perturbed SC, BCC, and FCC crystals are shown in Fig. 7 as a function of α. In all cases we find that $\langle\eta\rangle$ is larger than 3/2, with typical uncertainties of the order of at most $2 \cdot 10^{-3}$. Therefore $\langle\eta'\rangle$ is always larger than zero: such an anomalous scaling implies that, typically, a cell with a larger volume has a relatively smaller surface, and, in other terms, a larger isoperimetric quotient (which increases $\propto A^{2\eta'}$).

In particular, in the Poisson-Voronoi limit $\eta \approx 1.67$—black line in Fig. 6—which suggests the occurrence of a 5/3 exponent. It is also remarkable that, as soon as noise is turned on, anomalous scaling is observed for the SC and BCC cubic crystals. In the SC case, $\eta(\alpha = 0_+) \approx 1.88$, the exponent is monotonically decreasing for all values of α, and becomes undistinguishable from the Poisson-Voronoi limit for $\alpha > 2$. In the BCC case, as opposed to what one could expect given the structural stability of the crystal, $\eta(\alpha = 0_+) \approx 1.57 > 3/2$, which implies that a (modest) anomalous scaling is observed also for infinitesimal noise. The exponent increases for small values of α, overshoots the Poisson-Voronoi limit, and for $\alpha > 0.6$ its value basically coincides with what obtained in the SC case. When considering the FCC perturbed crystal, an anomalous scaling is observed for all finite values of noise, but, quite notably, $\eta(\alpha = 0_+) = 3/2$, which means that for infinitesimal noise anomalous scaling is not observed. So, in this regard, the FCC crystal seems to be more robust than the BCC one. In other terms, in the limit of vanishing noise (and of vanishing variability in the statistics of the areas and volumes of the cells) large cells tend to have a larger isoperimetric quotient in the perturbed SC and BCC crystals. Instead, in the perturbed FCC crystal such a selection does not take place: in this sense, shapes are better preserved.

As mentioned before, the number of faces provides a good proxy indicator for the shape of the cell, or, more precisely, of its isoperimetric quotient. In order to find a robust confirmation of the interpretation proposed for the presence of the anomalous exponent $\langle\eta\rangle > 3/2$ depicted in Fig. 7, we then attempt a power-law fit $V \propto A^{\eta}$ separately for each class of cells, each labeled with the number of faces. Therefore, for each value of the noise applied to the SC, FCC and BCC crystals, we obtain via best fit and ensemble averaging the estimate of the exponent $\langle\eta_f\rangle = 3/2 + \langle\eta'_f\rangle$ pertaining to the subset of cells having f faces. It is amazing (and re-ensuring) to find that for all cases considered $\langle\eta_f\rangle$ results to be lower that the corresponding "global" $\langle\eta\rangle$, so that we basically always have $\langle\eta'_f\rangle < 0.1$ (with typical uncertainties of the order of 10^{-2}), including when weak perturbation to the SC crystals are considered. We do not plot $\langle\eta_f\rangle$ as a function of α and f for the three perturbed crystals,

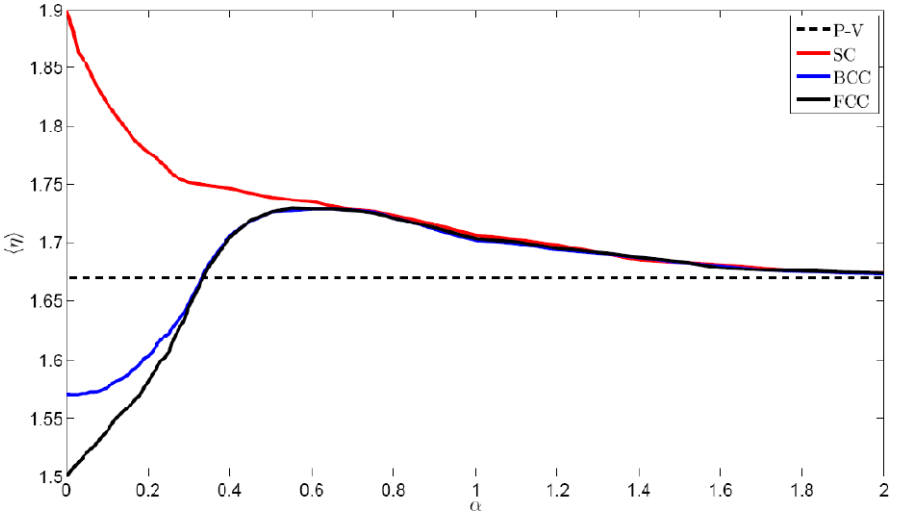

Fig. 7 Ensemble mean of the scaling exponent η fitting the power-law relation $V \propto A^{\eta}$ for the Voronoi cells of perturbed SC, BCC and FCC cubic crystals. The presence of an anomalous scaling ($\eta > 3/2$) due to the fluctuations in the shape of the cells is apparent. The error bars, whose half-width is twice the standard deviation computed over the ensemble, are too small to be plotted. The Poisson-Voronoi limit (see Fig. 6) is indicated. Details in the text

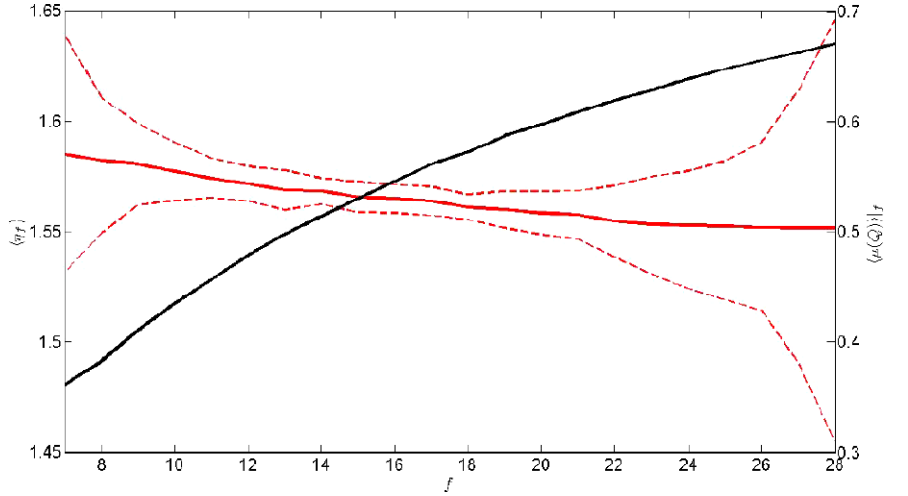

Fig. 8 Left y-axis, *red line*: Ensemble mean of the scaling exponent η fitting the power-law relation $V \propto A^{\eta}$ for cells with f faces of the Poisson-Voronoi tessellation. The range of f depicted in the figures covers over 99.9% of the cells. The *dashed lines* indicate $\pm$ twice the ensemble spread. Right y-axis, *black line*: Ensemble mean of the isoperimetric ratio for cells with f faces of the Poisson-Voronoi tessellation. The error bars, whose half-width is twice the standard deviation computed over the ensemble, are too small to be plotted. Details in the text

since what is obtained is just a plateau with no structure along the α or f directions. As an example, in Fig. 8 we plot $\langle \eta_f \rangle$ for the Poisson-Voronoi case. We observe that the anomalous scaling is greatly reduced and the deviation from the $3/2$ exponent is basically the

same independently of the value of f considered, even for very high and very low values of f, where the population of cells is rather scarce, and the ensemble spread is relatively large. The fact that within each f-class of cells the shape fluctuations are relatively small is confirmed by the negligible ensemble spread on the value of $\langle \mu(Q) \rangle|_f$. In agreement with what shown in Fig. 5, $\langle \mu(Q) \rangle|_f$ monotonically increases with f, thus indicating that each f-class of cell can be labeled in term of its isoperimetric quotient, with larger values of f corresponding to bulkier cells.

4 Summary and Conclusions

In this work we have studied the statistical properties of the 3D Voronoi tessellations generated by points situated on perturbed cubic crystal structures, namely the SC, BCC, and FCC lattices. This work is empirical and inductive, and wishes to stimulate further theoretical and numerical investigations.

The perturbations to the perfect crystal structures are obtained by applying Gaussian noise to the positions of each point. The variance of the position of the points induced by the Gaussian noise is expressed as $|\varepsilon|^2 = \alpha^2/\rho_0^{2/3}$, where α (which is a sort of square root of a normalized temperature) is the control parameter, ρ_0 is the number of points—and of Voronoi cells—per unit volume, and $\rho_0^{-1/3}$ is the resulting natural length scale. By increasing α, we explore the transition from perfect crystals to less and less regular structures, until the limit of uniformly random distribution of points is attained. Note that, for all values of α, the pdf of the lattice points is in all cases periodic. For each value of α, we have performed a set of simulations, in order to create an ensemble of Voronoi tessellations in the unit cube, and have computed the statistical properties of the cells.

The first notable result is that the Voronoi cells corresponding to SC and FCC lattices (cube and rhombic dodecahedron, respectively) are not stable in terms of topological structure. As soon as noise is turned on, their degeneracies—to be intended as non-generic properties of their vertices—are removed via a symmetry-break. With the introduction of an infinitesimal amount of noise, the pdf of the distribution of the number of faces per cell becomes smooth, with a finite standard deviation and a biased mean with respect to the zero noise case. Instead, the topological properties of the Voronoi cells (which are non-degenerate) of the BCC crystal are, as expected, stable against infinitesimal noise, so that the zero-noise limit of the Voronoi tessellation of the perturbed BCC structure is coincident with the unperturbed case. Nevertheless, it is surprising that the topology of the perfect BCC tessellation is robust also against small but finite noise. For strong noise, the statistical properties of the tessellations of the three perturbed crystals converge to those of the Poisson-Voronoi limit, but, quite notably, the memory of the specific initial unperturbed state is lost already for moderate noise, since the statistical properties of the three perturbed tessellations are indistinguishable already for $\alpha > 0.5$. As opposed to the 2D case, where hexagon is so overwhelmingly the "generic polygon", since hexagons constitute the stable tessellation, are the most common polygons of basically any tessellation, and the average number of sides of the cells is six [34], in the 3D case we do not have such a dominant topological structure.

Rather interesting features emerge looking at the metric properties of the cells, namely their surface area and their volume. Given the intensive nature of the Voronoi tessellation, the ensemble average of the mean and of the standard deviation of the area and of the volume of the cell scale as $\rho_0^{-2/3}$ and ρ_0^{-1}, respectively, so that we can easily obtain universal results by performing simulations with a specific given density ρ_0.

For all values of α, the standard deviation of the area of the Voronoi cells is basically the same for the three perturbed cubic structures: it features a linear increase for small noise, and then approaches asymptotically the Poisson-Voronoi limit for large values of α. Practically the same applies for the standard deviation of the volume of the cells.

Whereas the ensemble average of the mean volume is set to ρ_0^{-1} by definition, the analysis of the properties of the ensemble average of the mean area of the cells is quite insightful. In the case of perturbed BCC and FCC structures, the mean area increases only quadratically with α for weak noise, thus suggesting that the unperturbed Voronoi tessellation are local minima for the interface area. Instead, the mean area of the perturbed SC structure has a more interesting dependence on noise intensity: it decreases up to $\alpha \approx 0.3$, where a local minimum is attained, whereas for larger values of α, it increases until reaching the Poisson-Voronoi limit (as for FCC and BCC). So, counter-intuitively, noise can act as an "optimizer" in the case of the perturbed SC structure.

In all cases analyzed, 2-parameter gamma distributions are very effective in describing the empirical pdfs both for discrete variables, such as the number of faces, and for continuous variable, as in the case of the area and volume of the cells. Anyway, this issue requires a specific attention and specific results will be presented elsewhere.

In particular, in the case of Poisson-Voronoi processes, such an approach has been useful in analyzing statistically a controversy between an analytic result reported in [43] and [17] regarding the ensemble average of the mean number of sides per face in each Voronoi cell for a Poisson-Voronoi tessellation and the result of the numerical simulations presented in this paper. The discrepancy may be related to the definition of the appropriate probability measure to be used in the analytic integration; the analysis of such a disagreement deserves further, specific attention.

The presence of strong fluctuations in the area and volume of the Voronoi cells has suggested to check some joint area-volume statistical properties. In particular, we have considered the isoperimetric quotient Q, which measures the sphericity of the cells and is a good quantitative measure of the shape of the cells. The ensemble average of the mean value of Q is quadratic maximum for the FCC and BCC crystals for $\alpha = 0$, and, for any value of α, the perturbed BCC structure has the largest mean isoperimetric quotient. The observation that the truncated octahedron is a "large" local maximum for Q for space-filling tessellations suggests a weak re-formulation of the Kelvin conjecture of global optimality of the truncated octahedron, which has been proved false [57].

When noise in included in the system, Q features a certain degree of variability, which increases with noise. For a given amount of noise, such a variability is the smallest in the case of perturbed FCC structures, with BCC and SC structures coming next. The higher stability of the shape of the cells of the perturbed FCC structures is especially evidenced in the weak noise limit, where the standard deviation of Q vanishes quadratically with noise, whereas in the SC and BCC case such a decrease is only linear.

The investigation of the statistical properties of the shape of the cells can be taken from a slightly different point of view. When attempting a power law fit $V \propto A^{\eta}$ between the areas and the volumes of the Voronoi cells, we obtain with a very high degree of precision, for all perturbed tessellations, and for any intensity of noise, an anomalous scaling, i.e. $\langle \eta \rangle > 3/2$, with $\langle \eta \rangle \approx 1.67$ (suggesting a 5/3 exponent) in the Poisson-Voronoi limit. A positive anomaly $\langle \eta' \rangle = \langle \eta \rangle - 3/2$ is observed also for infinitesimal noise, except in the case of the perturbed FCC crystal, which, moreover, features the smallest anomaly in the exponent $\langle \eta' \rangle$ for all values of α, with, as above, BCC and SC coming next. These finding are connected to the properties of the fluctuations of the isoperimetric quotient mentioned above because the anomaly $\langle \eta' \rangle$ basically shows how large and small cells of the tessellation differ in their shape, since $\langle \eta' \rangle > 0$ indicates that large cells preferentially feature large

isoperimetric quotients ($Q \propto A^{2\eta'}$). Therefore, these results confirm that the Voronoi tessellation of the FCC crystal is the most stable in preserving the shape of the cells, even if it is topologically unstable. Note also that, basically because the isoperimetric quotient is strictly larger than zero and strictly lower than one, these scaling relations make sense only within a finite range of values of A and should be taken as descriptive of the bulk statistical properties of the cells.

In the simulations we find that the number of faces of a cell is a good proxy for its isoperimetric quotient: cells with a larger number of faces are typically bulkier. A further indication that the fluctuations in the shape determine the anomalous scaling between the areas and the volumes of the cells lies in the fact that the anomaly is greatly decreased when we classify the cells according to the number of their faces and attempt the power law fit class by class.

This work clearly defines a way of connecting, with a simple parametric control of spatial noise, crystal structure to uniformly random distribution of points. Such a procedure can be in principle applied for describing the "dissolution" of any crystalline structure. Our results emphasize the importance of analyzing in a common framework the topological and the metric properties of the Voronoi tessellations. We have shown that topological stability against weak noise does not necessarily correspond to metric stability for the shape of the cells, as measured by the isoperimetric quotient. Moreover, we have shown that, in order to grasp a better understanding, it is necessary to consider the joint statistical properties of the area and of the volume of the cells, thus going beyond 1D pdf. This has proved to be especially useful for framing in all generality the properties of optimality of the FCC and BCC structures.

Several open questions call for answers. The connection between the number of faces of the cells and their average isoperimetric quotient surely deserve further analyses. It would be important to analyze the impact of spatial noise on other relevant crystalline structures, such as the lattice whose Voronoi cell is the Weaire-Phelan structure. Moreover, since the perfect Hexagonal Close Packed (HCP) and FCC crystals are in close correspondence and agreement is found also when infinitesimal perturbations to the position of the points are considered [51], it would be interesting to compare extensively their statistical properties as finite noise of increasing amplitude is considered. Note that this analysis may provide some useful information regarding the well-known phase transition between white tin (HCP) and grey tin (FCC). The impact of noise on higher order statistical properties, such those of neighboring cells [46], should also be seriously addressed.

Finally, two additional important issues should be taken care of. First, some effort should be directed at addressing an issue that we have just briefly mentioned in the present paper, *i.e.* why, as shown in great detail in the literature, 2-parameter gamma distributions do such an amazing job in describing the pdfs of several geometrical properties of the Voronoi cells. A lot of references on this topic can be found in [43]. Some preliminary work at theoretical level, focusing on the exponential family of pdfs, is under way by C.T.J. Dodson and the author. Moreover, whereas most analyses aim at understanding the bulk statistical properties of the cells, it may be worthy changing the point of view and studying the statistical properties of the *extreme* cells by taking advantage of the approach based on Gnedenko's theorem [11].

Acknowledgements This paper is dedicated to F. Bassani (1929–2008), who played a fundamental role in stimulating the scientific curiosity of the author and specifically discussed with him the properties of SC, FCC, and BCC crystals. Moreover, the author wishes to thank G. Parisi, and C.T.J. Dodson for stimulating conversations, and the three anonymous reviewers for useful remarks which have greatly improved the quality of the paper.

References

1. Ashcroft, N.W., Mermin, N.D.: Solid State Physics. Saunders, Philadelphia (1976)
2. Aurenhammer, F.: Voronoi diagrams—a survey of a fundamental geometric data structure. ACM Comput. Surv. **23**, 345–405 (1991)
3. Averill, F.W., Painter, G.S.: Pseudospherical integration scheme for electronic-structure calculations. Phys. Rev. B **39**, 8115 (1989)
4. Barber, C.B., Dobkin, D.P., Huhdanpaa, H.T.: The quickhull algorithm for convex hulls. ACM Trans. Math. Softw. **22**, 469–483 (1996)
5. Barrett, T.M.: Voronoi tessellation methods to delineate harvest units for spatial forest planning. Can. J. For. Res. **27**(6), 903–910 (1997)
6. Bassani, F., Pastori-Parravicini, G.: Electronic States and Optical Transitions in Solids. Pergamon, Oxford (1975)
7. Bennett, L.H., Kuriyama, M., Long, G.G., Melamud, M., Watson, R.E., Weinert, M.: Local atomic environments in periodic and aperiodic Al-Mn alloys. Phys. Rev. B **34**, 8270–8272 (1986)
8. Bowyer, A.: Computing Dirichlet tessellations. Comput. J. **24**, 162–166 (1981)
9. Calka, P.: Precise formulae for the distributions of the principal geometric characteristics of the typical cells of a two-dimensional Poisson Voronoi tessellation and a Poisson line process. Adv. Appl. Probab. **35**, 551–562 (2003)
10. Christ, N.H., Friedberg, R., Lee, T.D.: Random lattice field theory: general formulation. Nucl. Phys. B **202**, 89–125 (1982)
11. Coles, S.G.: An Introduction to Statistical Modeling of Extreme Values. Springer, London (2001)
12. Desch, C.H.: The solidification of metals from the liquid state. J. Inst. Met. **22**, 241 (1919)
13. Dotera, T.: Cell crystals: Kelvin's polyhedra in block copolymer melts. Phys. Rev. Lett. **82**, 105–108 (1999)
14. Drouffe, J.M., Itzykson, C.: Random geometry and the statistics of two-dimensional cells. Nucl. Phys. B **235**, 45–53 (1984)
15. Du, Q., Wang, D.: The optimal centroidal Voronoi tessellations and the Gersho's conjecture in the three dimensional space. Comput. Math. Appl. **49**, 1355–1373 (2005)
16. Entezari, A., Van De Ville, D., Möller, T.: Practical box splines for reconstruction on the body centered cubic lattice. IEEE Trans. Vis. Comput. Graph. **14**, 313–328 (2008)
17. Finch, S.R.: Unpublished. Available on http://algo.inria.fr/csolve/vi.pdf. (2005). Addendum to Finch S.R.: Mathematical Constants. Cambridge University Press, Cambridge (2003)
18. Finney, J.L.: Volume occupation, environment and accessibility in proteins. The problem of the protein surface. J. Mol. Biol. **96**, 721–732 (1975)
19. Goede, A., Preissner, R., Frömmel, C.: Voronoi cell: new method for allocation of space among atoms: elimination of avoidable errors in calculation of atomic volume and density. J. Comput. Chem. **18**, 1113–1118 (1997)
20. Hales, T.C.: A proof of the Kepler conjecture. Ann. Math. **162**, 1065–1185 (2005)
21. Han, D., Bray, M.: Automated Thiessen polygon generation. Water Resour. Res. **42**, W11502 (2006). doi:10.1029/2005WR004365
22. Hentschel, H.G.E., Ilyin, V., Makedonska, N., Procaccia, I., Schupper, N.: Statistical mechanics of the glass transition as revealed by a Voronoi tessellation. Phys. Rev. E **75**, 50404(R) (2007)
23. Hilhorst, H.J.: Asymptotic statistics of the n-sided planar Poisson–Voronoi cell: I. Exact results. J. Stat. Mech. (2005). P09005 doi:10.1088/1742-5468/2005/09/P09005
24. Hinde, A.L., Miles, R.E.: Monte Carlo estimates of the distributions of the random polygons of the Voronoi tessellation with respect to a Poisson process. J. Stat. Comput. Simul. **10**, 205–223 (1980)
25. Hug, D., Schneider, R.: Typical cells in Poisson hyperplane tessellations. Discrete Comput. Geom. **38**, 305–319 (2007)
26. Hug, D., Reitzner, M., Schneider, R.: The limit shape of the zero cell in a stationary Poisson hyperplane tessellation. Ann. Probab. **32**, 1140–1167 (2004)
27. Icke, V.: Particles, space and time. Astrophys. Space Sci. **244**, 293–312 (1996)
28. Karch, R., Neumann, M., Neumann, F., Ullrich, R., Neumüller, J., Schreiner, W.: A Gibbs point field model for the spatial pattern of coronary capillaries. Physica A **369**, 599–611 (2006)
29. Kovalenko, I.N.: Proof of David Kendall's conjecture concerning the shape of large random polygons. Cybern. Syst. Anal. **33**, 461–467 (1997)
30. Kumar, S., Kurtz, S.K., Banavar, J.R., Sharma, M.G.: Properties of a three-dimensional Poisson-Voronoi tessellation: a Monte Carlo study. J. Stat. Phys. **67**, 523–551 (1992)
31. Isokawa, Y.: Poisson-Voronoi tessellations in three-dimensional hyperbolic spaces. Adv. Appl. Probl. **32**, 648–662 (2000)

32. Lewis, F.T.: The correlation between cell division and the shapes and sizes of prismatic cells in the epidermis of Cucumis. Anat. Rec. **38**, 341–376 (1928)
33. Li, S., Wongsto, A.: Unit cells for micromechanical analyses of particle-reinforced composites. Mech. Mater. **36**, 543–572 (2004)
34. Lucarini, V.: From symmetry breaking to Poisson point process in 2D Voronoi tessellations: the generic nature of hexagons. J. Stat. Phys. **130**, 1047–1062 (2008)
35. Lucarini, V., Danihlik, E., Kriegerova, I., Speranza, A.: Does the Danube exist? Versions of reality given by various regional climate models and climatological data sets. J. Geophys. Res. **112**, D13103 (2007). doi:10.1029/2006JD008360
36. Lucarini, V., Danihlik, R., Kriegerova, I., Speranza, A.: Hydrological cycle in the Danube basin in present-day and XXII century simulations by IPCCAR4 global climate models. J. Geophys. Res. **113**, D09107 (2008). doi:10.1029/2007JD009167
37. Luchnikov, V.A., Medvedev, N.N., Naberukhin, Yu.I., Schober, H.R.: Voronoi-Delaunay analysis of normal modes in a simple model glass. Phys. Rev. B **62**, 3181 (2000)
38. Meijering, J.L.: Interface area, edge length, and number of vertices in crystal aggregates with random nucleation. Philips Res. Rep. **8**, 270–290 (1953)
39. Miles, R.E.: A synopsis of Poisson flats in Euclidean spaces. In: Harding, E.F., Kendall, D.G. (eds.) Stochastic Geometry, pp. 202–227. Wiley, London (1974)
40. Møller, J.: Random tessellations in R^d. Adv. Appl. Prob. **21**, 37–73 (1989)
41. Møller, J.: Aspects of spatial statistics, stochastic geometry and Markov chain Monte Carlo. Aalborg, Aalborg University (1999)
42. Newman, D.: The Hexagon Theorem. IEEE Trans. Inf. Theory **28**, 129–137 (1982)
43. Okabe, A., Boots, B., Sugihara, K.: Spatial Tessellations—Concepts and Applications of Voronoi Diagrams, 1st edn. Wiley, West Sussex (1992)
44. Rapaport, D.C.: Hexagonal convection patterns in atomistically simulated fluids. Phys. Rev. E **73**, 025301 (2006)
45. Rapcewicz, K., Chen, B., Yakobson, B., Bernholc, J.: Consistent methodology for calculating surface and interface energies. Phys. Rev. B **57**, 007281 (1998)
46. Senthil Kumar, V., Kumaran, V.: Voronoi neighbor statistics of hard-disks and hard-spheres. J. Chem. Phys. **123**, 074502 (2005)
47. Sortais, M., Hermann, S., Wolisz, A.: Analytical investigation of intersection-based range-free localization information gain. In: Proc. of European Wireless (2007)
48. Soyer, A., Chomilier, J., Mornon, J.P., Jullien, R., Sadoc, J.F.: Voronoi tessellation reveals the condensed matter character of folded proteins. Phys. Rev. Lett. **85**, 3532–3535 (2000)
49. Tanemura, M.: Statistical distributions of Poisson-Voronoi cells in two and three dimensions. Forma **18**, 221–247 (2003)
50. Tanemura, M., Ogawa, T., Ogita, N.: A new algorithm for three-dimensional Voronoi tessellation. J. Comput. Phys. **51**, 191–207 (1983)
51. Troadec, J.P., Gervois, A., Oger, L.: Statistics of Voronoi cells of slightly perturbed face-centered cubic and hexagonal close-packed lattices. Europhys. Lett. **42**, 167–172 (1998)
52. Tsai, F.T.-C., Sun, N.-Z., Yeh, W.W.-G.: Geophysical parameterization and parameter structure identification using natural neighbors in groundwater inverse problems. J. Hydrol. **308**, 269–283 (2004)
53. Tsumuraya, K., Ishibashi, K., Kusunoki, K.: Statistics of Voronoi polyhedra in a model silicon glass. Phys. Rev. B **47**, 8552 (1993)
54. Voronoi, G.: Nouvelles applications des paramètres continus à la théorie des formes quadratiques. Premier mémoire: sur quelques propriétées des formes quadritiques positives parfaites. J. Reine Angew. Math. **133**, 97–178 (1907)
55. Voronoi, G.: Nouvelles applications des parametres continus a la theorie des formes quadratiques. Duesieme memoire: recherches sur les parallelodres primitifs. J. Reine Angew. Math. **134**, 198–287 (1908)
56. Watson, D.F.: Computing the n-dimensional tessellation with application to Voronoi polytopes. Comput. J. **24**, 167–172 (1981)
57. Weaire, D., Phelan, R.: A counter-example to Kelvin's conjecture on minimal surfaces. Philos. Mag. Lett. **69**, 107–110 (1994)
58. Weaire, D., Kermode, J.P., Wejchert, J.: On the distribution of cell areas in a Voronoi network. Philos. Mag. B **53**, L101–L105 (1986)
59. Yu, D.-Q., Chen, M., Han, X.-J.: Structure analysis methods for crystalline solids and supercooled liquids. Phys. Rev. E **72**, 051202 (2005)
60. Zhu, H.X., Thorpe, S.M., Windle, A.H.: The geometrical properties of irregular two-dimensional Voronoi tessellations. Philos. Mag. A **81**, 2765–2783 (2001)